

Studies on carotid plaque vulnerability using contrast enhanced ultrasound

Ola Hjelmgren

Department of Molecular and Clinical Medicine
Institute of Medicine
Sahlgrenska Academy at the University of Gothenburg



UNIVERSITY OF GOTHENBURG

Gothenburg 2015

Cover illustration: Carotid plaque imaging using B-mode ultrasound, contrast enhanced ultrasound, PET/CT and magnetic resonance imaging.

Studies on carotid plaque vulnerability using contrast enhanced ultrasound
© Ola Hjelmgren 2015
ola.hjelmgren@wlab.gu.se

ISBN 978-91-628-9575-4 (printed)
ISBN 978-91-628-9576-1 (epub)
<http://hdl.handle.net/2077/39555>

Printed in Gothenburg, Sweden 2015
Printed by Kompendiet Aidla Trading AB

“Allt som är lätt är redan gjort”

/ G. Bergström

Till Camilla och Hugo

Studies on carotid plaque vulnerability using contrast enhanced ultrasound

ABSTRACT

Background and Aim: Contrast-enhanced ultrasound is a method to examine neovessels that may be present inside the atherosclerotic plaque of the carotid arteries. These neovessels are believed to be involved in the process leading to embolic stroke. The aim of this thesis is to: I /Develop methodology for contrast-enhanced ultrasound examination of carotid plaques and to develop a software program for quantification of the examination. II /Investigate the correlation between neovessels and inflammation in plaques, using PET/CT. III / Investigate the correlation between neovessels and plaque components using MRI. IV / Comparing ultrasound and MRI in detecting and measuring of carotid plaques.

Methods: The papers of this thesis are performed on volunteers recruited through several different databases. The contrast-enhanced ultrasound method has been developed and optimized within the framework of the thesis. For comparison, conventional ultrasound, PET / CT and MRI has been used.

Results: The method we have developed for contrast-enhanced ultrasound is reproducible and reliable. Increased amount of neovessels is more common in subjects with a history of stroke or transient ischemic attack and neovessels are correlated to increased inflammation. Neovessels are less common in plaques with a large lipid-rich necrotic core. Two dimensional imaging using ultrasound does not correctly capture the complex 3D plaque anatomy. MRI is comparable to ultrasound in finding plaque with a height of at least 2.5 mm, but in detection of smaller plaques ultrasound performs better. Multiple plaques seen on ultrasound are usually a misinterpretation of the true anatomy that can be better visualized using MRI. Plaque height measured using ultrasound is slightly more accurate and more feasible than plaque area to estimate the plaque volume measured using MRI.

Conclusion: Contrast-enhanced ultrasound can be used to measure and quantify neovessels in carotid plaques. The quantity of neovessels correlates with the degree of inflammation, a marker for plaque vulnerability. However, the size of the lipid core, another marker of plaque vulnerability, has an inverse correlation to neovessels. Future studies should in more detail examine the exact localization of neovessels in relation to the lipid core. Also, future studies should examine the quality of neovessels since they can

have different propensity to cause damage. Small plaques can be undetectable by MRI but in plaques greater than 2.5 mm in height, ultrasound and magnetic resonance imaging have similar sensitivity to detect plaques. If using ultrasound, plaque height is the best way to estimate the volume of the carotid artery plaque.

Keywords: Atherosclerosis, Carotid artery plaque, Contrast-enhanced ultrasound, Positron-emission tomography, Magnetic resonance imaging

ISBN 978-91-628-9575-4 (printed)

ISBN 978-91-628-9576-1 (epub)

<http://hdl.handle.net/2077/39555>

SAMMANFATTNING PÅ SVENSKA

Bakgrund: Kontrastförstärkt ultraljud är en metod för att undersöka små blodkärl (mikrokärl) som kan finnas inuti åderförkalkningsplack i halskärlen. Dessa mikrokärl är troligen inblandade i förloppet som leder till att placket orsakar stroke. Avhandlingens mål att: I/ Utveckla metodik för att med kontrastförstärkt ultraljud undersöka halskärlsplack och att utveckla mjukvara för att analysera undersökningen. II/ Undersöka sambandet mellan mikrokärl och inflammation i plack, där inflammationen mäts med ett spårämne i en PET/CT-kamera. III/ Undersöka sambandet mellan mikrokärl och plackets övriga beståndsdelar. Analysen av beståndsdelar görs med magnetkamera. IV/ Jämföra ultraljud och magnetkamera för att se hur bra teknikerna är på att hitta, avbilda och mäta plack i halskärlen.

Metoder: Delarbetena i avhandlingen är utförda på frivilliga försökspersoner som rekryterats via flera olika databaser och är väl karakteriserade. Tekniken för kontrastultraljud har utarbetats och optimerats inom ramen för avhandlingen. För jämförelse har konventionellt ultraljud, PET/CT och magnetkamera använts.

Resultat: Den metod vi utvecklat för kontrastförstärkt ultraljud är reproducerbar och tillförlitlig. Ökad mängd mikrokärl är vanligare hos de som tidigare drabbats av stroke eller övergående stroke och mikrokärl är kopplat till ökad inflammation. Ökad mängd mikrokärl är också kopplat till en mindre lipidkärna. Konventionellt ultraljud fångar inte plackets anatomi som är komplex och kräver tredimensionell avbildning. Magnetkamera är jämförbart med ultraljud när det gäller att hitta plack som är minst 2,5 mm höga men vid mindre plack presterar ultraljud bättre. När man på ultraljud ser flera plack i ett kärl är detta oftast en feltolkning av anatomin. Plackhöjd är mer användbart än plackarea för att uppskatta plackstorlek med ultraljud.

Slutsatser: Kontrastförstärkt ultraljud kan användas för att mäta förekomsten av mikrokärl i halskärlsplack. Förekomsten av mikrokärl är kopplat till graden av inflammation, en markör för att placket är eller kan bli farligt och leda till stroke. Dock är lipidkärnans storlek, en annan markör för farlighet, mindre när antal mikrokärl ökar. Potentiellt farliga mikrokärl kan finnas på speciellt utsatta ställen i placket och framtida studier bör inriktas på detta och på mikrokärlens kvalitet. Mindre plack kan vara omöjliga att upptäcka med magnetkamera men vid plack större än 2,5 mm är ultraljud och magnetkamera jämförbara. Plackhöjd är det mest användbara sättet att mäta storleken på halskärlsplack vid ultraljud.

LIST OF PAPERS

This thesis is based on the following studies, referred to in the text by their Roman numerals.

- I. Hjelmgren O, Holdfeldt P, Johansson L, Fagerberg B, Prah U, Schmidt C, Bergström G ML. Identification of Vascularised Carotid Plaques Using a Standardised and Reproducible Technique to Measure Ultrasound Contrast Uptake. *Eur J Vasc Endovasc Surg.* 2013;46(1):21-8.
- II. Hjelmgren O, Johansson L, Prah U, Schmidt C, Fredén Lindqvist J, Bergström G ML. A study of plaque vascularization and inflammation using quantitative contrast-enhanced US and PET/CT. *Eur J Radiol.* 2014;83(7):1184-9.
- III. Hjelmgren O, Johansson L, Prah U, Schmidt C, Bergström G ML. Inverse Association Between Size of the Lipid-Rich Necrotic Core and Vascularization in Human Carotid Plaques. Submitted.
- IV. Hjelmgren O, Schmidt C, Johansson L, Bergström G ML. Comparison between magnetic resonance imaging and B-mode ultrasound in detecting and estimating the extent of human carotid atherosclerosis. Manuscript.

Reprints were made with permission from the publishers.

CONTENT

ABBREVIATIONS	5
1 INTRODUCTION	7
1.1 Atherosclerotic disease.....	7
1.1.1 Risk factors	8
1.1.2 Plaque localization.....	9
1.2 The vulnerable plaque	9
1.3 Neovascularization – a possible marker of vulnerability	10
1.4 Imaging methods	11
1.4.1 Ultrasound	12
1.4.2 Ultrasound in carotid plaques	12
1.4.3 Contrast enhanced ultrasound, CEUS	13
1.4.4 CEUS in carotid plaques	14
1.4.5 Magnetic resonance imaging, MRI	16
1.4.6 MRI of Carotid plaques	17
1.4.7 PET/CT	18
1.4.8 Spatial resolution of the different imaging modalities	19
2 AIM	21
3 PATIENTS AND METHODS	23
3.1 Subjects	23
3.2 Paper I – Evaluation of CEUS.....	23
3.2.1 Development of CEUS protocol.....	23
3.2.2 Development of the CQP.....	24
3.3 Paper II – CEUS and inflammation.....	24
3.4 Paper III – CEUS and LRNC	25
3.5 Paper IV - Detection of plaques	25
3.6 Ethical considerations	25
3.7 Statistics	26
4 RESULTS	27

4.1	Paper I – Evaluation of CEUS.....	27
4.2	Paper II – CEUS and inflammation.....	28
4.3	Paper III – CEUS and LRNC	29
4.4	Paper IV – Detection of plaques.....	30
5	DISCUSSION	31
5.1	Major findings in Paper I-III	31
5.1.1	Applicability of CEUS.....	34
5.1.2	Quantification of CEUS.....	34
5.2	Differences between 2D ultrasound and MRI – Paper IV.....	35
6	CONCLUSION.....	39
7	FUTURE PERSPECTIVES	41
	ACKNOWLEDGEMENT	43
	REFERENCES	44

ABBREVIATIONS

CEUS	Contrast Enhanced UltraSound
LDL	Low Density Lipoprotein
LRNC	Lipid-Rich Necrotic Core
IPH	Intra Plaque Hemorrhage
IMT	Intima-Media Thickness
GSM	Grey Scale Median
MI	Mechanical Index
TIA	Transient Ischemic Attack
CPS	Contrast Puls Sequencing
MES	Micro Embolic Signals
MRI	Magnetic Resonance Imaging
TOF-MRA	Time Of Flight Magnetic Resonance Angiography
MP-RAGE	Magnetization-Prepared Rapid Acquisition Gradient Echo
PET/CT	Positron Emission Tomography/Computer Tomography
FDG	Fluor-DeoxyGlucose
SUV	Standard Uptake Value
CQP	Contrast Quantification Program
TBI	Tissue Background Index

1 INTRODUCTION

The main aim of this thesis is to study contrast enhanced ultrasound, CEUS, as a potential method to visualize and quantify neovascularization of carotid plaques. The basic concept is to detect neovascularization inside the plaques since presence of such vessels could be a sign of a vulnerable plaque, prone to cause disease. However, the pathophysiological significance of neovessels in carotid plaques and their role in the development leading to stroke is not fully known. There is clearly a need for better imaging methods to study plaque composition *in vivo*.

1.1 Atherosclerotic disease

Cardiovascular disease is a leading cause of death and morbidity throughout the world(1). The most common clinical presentations are myocardial infarction and stroke and the underlying pathology of both presentations is the atherosclerotic disease process in the vessel wall. In general, the arterial vessel wall consists of three layers. The outer layer, tunica adventitia, consists of connective tissue. In larger vessels the adventitia may have nerve fibers and small blood vessels (vasa vasorum) for the internal nutrient support of the vessel wall. The middle layer, tunica media, consists primarily of circumferential layers of smooth muscle cells. The inner layer, the intima, has a monolayer of endothelial cells towards the blood. The endothelium is resting on a basal lamina and a sub endothelial layer of loose connective tissue(2). The oxygen supply to the intima and media are in the healthy vessel mainly supplied by oxygen diffusion with very few blood vessels(3).

The development of atherosclerosis is a slow process over several decades and the steps of the process, in particular the early steps, are difficult to study in humans.

In the response-to-retention hypothesis(4), the atherosclerotic process starts with retention and accumulation of small lipoprotein inside the intima. These small lipoproteins, like low density lipoprotein (LDL), can cross an intact endothelium and the majority of LDL diffuses through the arterial wall, only a minority is trapped, or retained. The retention mainly occurs because lipoproteins are bound to proteoglycans in the extra cellular matrix(4). Oxidation of the retained lipids induces local cytokine release and the cytokines attract monocytes to enter the intima, differentiate into

macrophages and start taking up the oxidated lipids. After doing this, the macrophages are called foam cells(5).

Foam cells also work as inflammatory activators through a number of different pathways. T-cells are recruited and can promote apoptosis of smooth muscle cells, endothelial cells and macrophages. If the atherosclerotic process continues, a lipid-rich necrotic core (LRNC) develops in the intima. The LRNC is an accumulation of acellular material containing lipid rich material and cholesterol crystals. This material is derived from foam cells and smooth muscle cells. Apoptosis of foam cells and smooth muscle cells can be seen in the margins of the LRNC. Since the remnants are not removed by phagocytes, the lipid rich cargo deposited in the tissues increase the size of the LRNC(6,7).

Smooth muscle cells are rarely found in the normal intima but as the lesion grows, their number increases (8). Smooth muscle cells migrate from the media layer into the intima where they divide and expand the extracellular matrix of collagen and proteoglycan. The connective tissue gradually changes from normal, loose tissue into a collagen-rich fibrous tissue(9).

With increasing age, parts of the plaque can be calcified. The process can begin with microscopic calcium granule that form and gradually expand into larger lumps and plates, more often seen at the base of the LRNC close to the media(10). The mechanisms behind calcification is poorly understood(11) and the predictive value of calcification is debated(12).

As the plaque grows, diffusion distances for oxygen and nutrients increase and the plaque develops its own microcirculation, the neovascularization of the plaque(13). The neovessels may allow further growth of the plaque but they also may be fragile and prone to rupture(14). A rupture would lead to bleeding inside the plaque called intra plaque hemorrhage (IPH).

1.1.1 Risk factors

Large-scale epidemiological studies, like the Framingham study, established a number of important risk factors for development of cardiovascular disease(15). The conventional risk factors age, male sex, smoking, hyperlipidemia, hypertension and diabetes have all shown to increase the risk of cardiovascular events on a group level. Preventive medicine, aimed at reducing these risk factors has been a great success in modern medicine, lowering the morbidity and mortality in cardiovascular disease(16). However, these risk factors lack precision for the individual and also in the timing of cardiovascular disease(17). In the future, it is hoped that the

combination of traditional risk factors, new biomarkers of disease and image-derived information will improve this situation(18).

1.1.2 Plaque localization

Risk factors like smoking, hyperlipidemia and diabetes affect all parts of the vascular tree similarly. Despite this, atherosclerosis is not equally distributed throughout the circulation. Atherosclerotic plaques are most common directly after artery branches, and they are rare in parts of vessels without branches. One theory is that the turbulent flow in branches exposes the endothelial cells to less shear stress, making them more permeable for atheroma inducing agents(19,20).

1.2 The vulnerable plaque

As the plaque grows larger it will gradually affect blood flow. A clinical presentation of this is stable angina(21). In the cerebral circulation the stable, partly occluding carotid plaque is seldom a clinical problem since the brain has a well developed collateral blood circulation. Perfusion of the brain is usually fully compensated if one of the four vessels to the brain is occluded. The plaque in the carotid artery can therefore be clinically silent and may in fact never result in disease(22).

However, when a thrombus is formed on the plaque a much more dramatic series of events can occur. In the heart, a thrombus on a plaque in a coronary artery can suddenly occlude the coronary artery and result in myocardial infarction(23,24). A plaque rupture in the carotid artery can form a local thrombus that causes a stroke via embolization to the cerebral circulation (24). The mechanism behind formation of thrombi is believed to be rupture of the fibrous cap of the plaque and exposure of thrombogenic material like lipids and extracellular matrix constituents to the flowing blood and its coagulation system(5). Plaque rupture has long been believed to be the main mechanism for cardiovascular events. A lesser part of events is believed to be caused by superficial erosion, where only the endothelial layer of the plaque is damaged(5). However, recent data suggest that there is a shift in the pathophysiology of the disease towards less events on the basis of plaque rupture, and more events from superficial plaque erosion(25).

The mechanism leading from a stable plaque to plaque rupture are not clearly elucidated. Observational data mainly come from histological studies on autopsy and surgical specimens(5,26) and there is a lack of longitudinal studies of plaque biology using imaging. In the prevailing theory, the

macrophages in atheroma overexpress matrix degrading proteases (i.e. metalloproteinases) that degrade the extracellular matrix, making the fibrous cap weaker(5,27). The degree of inflammation in the intima is thus linked to the stability of the plaque(28). Increased inflammation can also induce increased cell death of smooth muscle cells, lowering the production of extracellular matrix resulting in a thinner fibrous cap with less collagen (29) and a larger LRNC, both mechanically destabilizing the plaque. A large lipid pool inside the plaque could increase the degradation of matrix proteins and a large central lipid core could increase the mechanical forces on the shoulder regions of the plaque(30). Hence, a large LRNC, a thin cap and accumulation of inflammatory cells are all thought to be signs of plaque vulnerability increasing the likelihood of plaque rupture(5). The mechanisms behind superficial plaque erosion are less well described, however, these plaques seem to have a smaller lipid core and less of inflammatory activity(31).

1.3 Neovascularization – a possible marker of vulnerability

In normal arteries, the intima and inner media is supported with nutrients and oxygen by diffusion from the vessel lumen(32). Deeper parts of the media and the adventitia are supported from neovessels extending from the vasa vasorum. Observational data shows that as the vessel wall thickens, when the atherosclerotic lesion grows, neovessels grow into the thickening intima, mainly from the vasa vasorum, and only rarely from the vessel lumen(33). More neovessels are seen in lipid-rich lesions, in lesions with dense macrophage infiltration of the fibrous cap and in lesions with a thin cap(33,34). It is proposed that hypoxia inside the plaque stimulate the neovascularization and as the thickness of the lesion grows, hypoxia in the deeper parts of the intima stimulate neovessels to form(13), but also the increased oxygen consumption of the macrophages could generate hypoxia (32,35). Cytokine release from local inflammatory activity induced by macrophages, T-cells and mast cells in the intima, further stimulate this process. It is also proposed that hypoxia stimulates inflammation(36), recruiting even more monocytes. Hypertension induced stress on smooth muscle cells, oxidative stress and nicotine has also been proposed to stimulate neovascularization(34). The neovessels seen in atherosclerotic disease are enlarged and disorganized with irregular vessel diameters compared to the micro vessels seen in normal arteries (37) and they are described as leaky with less developed junctions between their endothelial cells(14,38). Neovessels are more common in the shoulder regions and in the base of the plaque and are co-localized with inflammatory cells(39). Cross

sectional studies shows that the neovessels are associated with more severe plaque phenotypes and with inflammatory activity. Also, neovessels are more common in symptomatic plaques(37). Other studies indicate that presence of neovessels could indicate an increased risk of cardiovascular events(40). It is unclear if the neovessels can reduce the hypoxia, in fact it has been proposed that the neovessels lack the capability of delivering sufficient oxygen for nutrition(36). However, they enable inflow of more monocytes into the plaque, thereby creating a vicious circle of hypoxia and inflammation(36,41).

The endothelial surface of the neovessels in a highly vascularized plaque is much greater than the endothelial surface facing the vessel lumen(34). Therefore it has been proposed that the plaque mainly is supported with oxygen and nutrients through these vessels(33,42). In observational studies, presence of neovessels correlates spatially with presence of increased inflammation(39). From these studies, it is not possible to know if the inflammatory cells are delivered by the vessels or if vessel growth were stimulated by prevailing inflammation(34).

Intra plaque hemorrhage (IPH) is identified as a mechanism leading to a vulnerable plaque prone to rupture(6,43). The bleeding seems to come from the neovessels, not the vessel lumen(6,44). Higher levels of matrix metalloproteinase have been found close to the neovessels and it has been proposed that the vessels thereby could be weakened and prone to rupture and bleeding(32). The IPH deposits large amounts of red blood cells in the plaque, which is metabolized into large amounts of free cholesterol. Cholesterol and red blood cells will be phagocytized by macrophages leading to further necrotic core expansion(6,33). In cross-sectional studies, plaque hemorrhage is associated with increased number of neovessels(37).

The role of neovascularization has been described as dual(32). In the earlier stages the neovessels stabilizes the plaque. Later, the inflammatory cells release matrix metalloproteinases and other substances that degrade the neovessels and make them prone to rupture and cause IPH, thereby making the plaque vulnerable(32).

1.4 Imaging methods

Plaques in the carotid arteries may rupture and cause embolic stroke, and this probably accounts for 15% of all stroke cases(45). The carotid atherosclerotic disease occurs in the proximal part of the internal carotid artery. Plaques at this site are accessible for different non-invasive imaging methods, which makes them suitable for studies on plaque biology and disease mechanisms.

1.4.1 Ultrasound

Ultrasound is a widespread technology in examining vascular function and morphology and typically uses frequencies between 1 and 20MHz. B-mode ultrasound is the standard technology for making real-time 2D, or 3D, images. Sound waves (mechanical waves) are sent into the tissue, and are partially reflected every time it passes border surfaces between different tissues. The propagation of the sound wave depends on acoustic impedance, and the acoustic impedance (Z) of a material is defined as the product of its density (ρ) and acoustic velocity (v), $Z = \rho \cdot v$. The amount of sound wave reflected depends on the change in acoustic impedance between the different tissues and on the angle between the ultrasound beam and the interface. Optimal reflection occurs at 90 degrees(46).

If the structure is smaller than the wavelength of the ultrasound, scattering occurs, where the energy is radiated in all directions, and only a small amount comes back to the transducer. In ultrasound, pulses of sound are sent into the tissue. From time elapsed until the echo returns the distance to the echo is calculated, and an image is presented. The image signal is processed in the ultrasound system in a number of steps, many of them proprietary to the vendor and not disclosed to the operator. In general, the brighter an object appear on the screen, the stronger the signal of the echo. The image is usually made of pixels coded in 256 steps from black to white.

Modern ultrasound can also use tissue harmonic imaging, where small tissue elements resonate from the sound wave, and produce second harmonic tones, a tone in a higher octave. The returned signal is processed and the fundamental frequencies are filtered away. An image made from harmonic echoes instead of the fundamental echoes has advantages in some cases since it lowers the noise(47).

B-mode ultrasound imaging can be used to detect plaques of different sizes visually and, using Doppler, the blood velocity can be measured which is widely used to determine degree of stenosis. Blood flow velocities are not increased until 50% of the lumen is obstructed by plaque tissue(48).

1.4.2 Ultrasound in carotid plaques

In clinical practice as well as in research, carotid plaques are primarily detected with ultrasound. To define a plaque on ultrasound there is the well-accepted Mannheim consensus(49). The intima itself cannot be measured using ultrasound but the adventitia can be separated from the two inner layers, hence the description Intima-media-complex. In the Mannheim

consensus a plaque is defined as focal structure encroaching into the arterial lumen at least 0.5 mm or 50% thicker than the surrounding intima-media thickness (IMT), or demonstrates a thickness >1.5 mm as measured from the media-adventitia interface to the intima-lumen interface(49).

Plaque echogenicity

Carotid plaques have different appearances in the ultrasound gray-scale image, from low echogenic (dark) to high echogenic (bright). Sometimes the plaques are heterogeneous in their echogenicity. Classification of plaque echogenicity on ultrasound have been made visually on a reproducible and standardized nominal scale named after its inventor, Gray-Weale(50). The Gray Scale Median (GSM) is a way to objectively measure the echogenicity of the plaque in the ultrasound image using a standardization of the pixel image values. Values are linearly scaled most often using blood and adventitia as references(51-53). The median pixel value inside the plaque is called GSM. Low echogenicity (hence low GSM) is associated with high content of lipid and blood(51,54-58). A few prospective studies suggest that subjects with low-echogenic plaques have higher risk for future events(59,60).

1.4.3 Contrast enhanced ultrasound, CEUS

Contrast-enhanced ultrasound (CEUS) uses a specific intravascular contrast agent consisting of micro bubbles. The micro bubbles are gas filled vesicles with a phospholipid shell. In this thesis, the second-generation ultrasound contrast agent SonovueTM (Bracco Imaging, Milan, Italy) was used. The SonovueTM micro bubbles are small, the mean diameter is 2.5 micrometer, and are filled with sulfur hexafluoride gas. Sulfur hexafluoride is an inert high-density gas and the high molecular weight of the gas inside the bubbles slows down the diffusion of gas out of the bubble. This makes the bubbles survive longer in the bloodstream in comparison to first generation contrast agents that were using air. The contrast agent is strictly intravascular; the bubbles cannot leave the blood vessels. Contrast bubbles are injected in a vein and small enough to pass the pulmonary circulation. When the bubbles burst, the gas is cleared through the lungs and exhaled. SonovueTM has been widely used in clinical examinations, mostly tumor diagnostics in the liver. The safety is well documented, with an incidence of severe adverse reaction in approximately 1 in 10 000(61).

The size of the bubbles are carefully chosen so that their resonance frequency is close to the fundamental frequency of diagnostic ultrasound. When the bubbles are hit by the ultrasound wave they start to oscillate, and will both

absorb and scatter ultrasound with high efficiency. This makes the echo from micro bubbles much stronger than tissue echoes.

The mean size of the micro bubbles is 2.5 micrometer. The diameter of carotid plaque neovessels range from 2-200 micrometers(36) when measured as smallest diameter. In our own histologic examinations of carotid plaques, the majority of micro vessels range from 3 to 150 micrometers in diameter, however, some subjects have larger micro vessels with a diameter 500-800 micrometer.

Mechanical index

Mechanical index (MI) expresses the power from the ultrasound beam on the tissues. It is defined as the peak negative pressure divided by the square root of the center frequency of the ultrasound wave. With an MI of 1.2 or higher the bubbles break. In CEUS of carotid plaques, a low MI is used. In our studies we used an MI around 0.06 to ensure the integrity of the bubbles.

Contrast Pulse Sequencing

When the contrast-agent bubble is hit by a sonic wave, the gas expands more easily than it compresses. This behavior is different from the behavior of tissue. This behavior is called non-linear motion and leads to the rich production of harmonic overtones from the bubbles. Using this phenomenon it is possible to filter out and separate the signal from the bubbles from the signal originating from surrounding tissue. By sending out trains of pulses and changing the amplitude and phase of the ultrasound pulse, the returning echoes from tissue and bubbles can be separated with great accuracy. In this thesis the Cadence Contrast Pulse Sequencing (CPS) software program, by Siemens, was integrated in the ultrasound system(62).

1.4.4 CEUS in carotid plaques

Efforts have been made to develop CEUS for detection of neovascularization in carotid plaques in vivo. The ultimate goal would be to use CEUS and the quantification of neovascularization to risk-stratify individuals with carotid plaques into stable or vulnerable. The technique could also be used to monitor the effect of various treatments aimed at reducing plaque vulnerability.

Today (19 September, 2015) there are, to our knowledge 27 original research publications in English on the topic, including our own 2 published works.

Neovascularization assessed with CEUS and histologic verification

At present there are 13 studies comparing data from CEUS with histology in carotid plaques(63-75). They are all rather small, however these studies clearly indicate that increased signal from contrast agent inside carotid plaques is a marker of neovascularization. There is no standardized method on how to conduct a CEUS examination of a carotid plaque. Also, there is no consensus about how to quantify the result of the examination.

CEUS and history of stroke or transient ischemic attack

At present there are 10 papers that have studied the relationship between neovascularization assessed by CEUS and history of earlier cerebral symptoms, such as ipsilateral stroke or transient ischemic attack (TIA). Seven of these studies, including our own work and two of the largest studies by Huang and Xiong, found an association(66,68,70,76-79). Three studies did not find such an association(72,74,80).

Neovascularization and micro embolic signals

Two studies have compared the presence of micro embolic signals (MES) on transcranial Doppler examination and plaque neovascularization(80,81). MES positive subjects are thought to suffer from sub-clinical micro emboli to the cerebral circulation(82). Both studies show increased neovascularization in subjects that are MES positive.

Neovascularization and echogenicity

Excluding our own work, CEUS has been correlated with the plaque echogenicity in six published studies. In three of these studies echogenicity is measured with GSM(66,70,78). These studies show an inverse correlation between GSM and neovascularization but they do not address the problem with acoustic shadowing when using CEUS. Five studies compare neovascularization with echogenicity visually classified on various nominal scales(42,65,73,76,83). In two of these studies, no correlation is seen(42,73). In the remaining three studies the authors find an inverse association, Xiong et al conclude that this finding could be false(76), since calcifications can shadow the ultrasound contrast agent. Coli et al(65) reports that 25% of plaques have extensive calcification with acoustic shadowing but this finding is not considered as a bias. Huang et al(83) uses a different classification of echogenicity, however, these authors do not consider acoustic shadowing as a bias.

Quantification of CEUS

The first studies comparing CEUS to histology used a visual scale to grade neovascularization(63-66). Various commercially available software programs have been used to plot time intensity curves to measure the enhancement of mean intensity inside the plaque compared to the enhancement in lumen(68-73,75). Two recent studies comparing CEUS to histology have used more advanced and dedicated software programs(67,74). Two studies have chosen to analyze late-phase images, six minutes after contrast agent injection(69,78).

Pseudo enhancement

The bubbles in the vessel lumen could give a mirror artifact in structures of the far wall. Plaques in this location could appear brighter on CEUS without having more micro vessels(84,85).

1.4.5 Magnetic resonance imaging, MRI

Magnetic resonance imaging (MRI) uses the hydrogen nucleus, a proton, to make images. Using strong magnetic fields and energy in the radiofrequency range the hydrogen nucleus can produce different signals depending on what tissue it is surrounded by.

When put inside a strong magnetic field the protons align their directions parallel or anti-parallel with the surrounding magnetic field, with a slight predominance of parallel alignment. The spinning protons act as small magnets and when a radio frequency pulse is applied, all these small magnets move in phase, and their magnetization can be recorded as a current in a receiver coil. The direction of the magnetization can be described as a vector, called the net magnetization vector.

There are different ways to produce MR images. T1 relaxation time is the time for a proton in a certain tissue to restore the longitudinal part of the net magnetization vector. When the radio frequency pulse is turned off, the protons will gradually decay back to a lower energy state. Fat can easily absorb energy from the surrounding protons, and this makes the process faster and the T1 in fat is therefore short. Water on the other hand cannot absorb energy at the same speed. If the recording of signal from the coil is made before all tissues have gone back to their original state, there will be differences in the signals originating from differences in T1 between fat and water where fat shows a higher signal. Gadolinium contrast agents are water-soluble agents that lower the T1 time of the surrounding protons.

T2 relaxation time is the time it takes for the horizontal component of the net magnetization vector to dephase. Also T2 decay occurs faster in fat than in water, mainly because the hydrogen nucleuses of fat are more dense packed in fat compared to water, which makes the interactions from surrounding atoms higher(86).

1.4.6 MRI of Carotid plaques

High-resolution magnetic resonance imaging of carotid arteries (MRI) is an imaging technique where the use of a dedicated surface coil enables high resolution imaging of the carotid arteries in a small field of view around the carotid bifurcation. The main strength of MRI is the possibility to assess and quantify plaque components(87-91). It has also been reported that it is possible to identify an intact fibrous cap (89,92,93). The most interesting target for MRI is probably the ability to identify intra plaque hemorrhage (IPH). Decomposition of blood accumulated in the plaque turns the blood into methemoglobin which results in T1-shortening and hence a strong signal on T1 weighted sequences(94). Subjects with IPH have a higher risk for future events compared to subjects with plaques that do not show IPH(43,95). The following sequences are commonly used.

Time of flight MR-angiography, TOF-MRA

TOF-MRA is a sequence that can visualize the artery lumen without the need of intravasal contrast agent. Basically the stationary tissue is subject to repeated radio frequency pulses that eventually will turn the net magnetization vector close to 0 degrees which is called saturation(86). TOF-MRA can be used to detect plaque ruptures(92,93,96). However, in MRI of carotid plaques it is difficult to know if high signal inside a plaque originates from IPH or rupture that brings arterial blood into the plaque.

Quadruple inversion recovery

An inversion recovery sequence makes it possible to null the signal from a certain tissue. A pre-pulse is timed before the radio frequency pulse so that the desired tissues have reached zero magnetization. The sequence is then started and the desired tissue will not generate any signal. This is one of the ways in which for example the signal from fat can be eliminated. In the quadruple inversion recovery sequence there are four pre-pulses. First a non slice-selective 180-degree pulse then a 180-degree slice selective pulse. Tissue and blood outside as well as inside the slice will be nulled by the first 180-degree pulse, tissue and blood inside the slice will be restored by the second pulse. This is done twice before the reading is done. When the reading is done, the blood has moved and nulled blood will be inside the slice

and appear black. By doing the inversion two times before the reading, the quadruple inversion recovery sequence will null blood in a wide range of T1. The same sequence will therefore null blood before and after administration of gadolinium. This makes it possible to compare pre and post gadolinium images and quantify the contrast enhancement(97). The sequence we used also contained a fat-saturation, reducing the signal from subcutaneous fat. LRNC has a different fat composition than subcutaneous tissue, T2 in LRNC is short and this makes the signal from LRNC weak. The inversion recovery sequence in combination with gadolinium contrast is therefore very suitable for outlining the LRNC(89-91).

MP-RAGE

IPH deposits blood in the plaque. The Hemoglobin is then transformed into methemoglobin. Methemoglobin has short T1 and appears bright on T1 weighted images. A magnetization-prepared rapid acquisition gradient echo (MP-RAGE) is a highly T1-weighted sequence that has been shown to result in a high detection rate for IPH in plaques. MP-RAGE is better than TOF-MRA and fast spin echo sequences(94,98). Coexisting calcifications, especially scattered ones, will however lower the signal from IPH.

1.4.7 PET/CT

Positron emission tomography (PET) is based on imaging using molecular positron emitting tracers. The most common tracer is fluor-18 attached to a modified glucose molecule, Fluor-DeoxyGlucose (FDG). FDG is a glucose analog and behaves like glucose in the human body. After entering glycolysis it is phosphorylated but is then trapped inside the cell since it cannot be further metabolized. Fluor-18 has a half-life of 109 minutes; it decays and releases a positron which interacts with tissue and two photons are released. The PET-scanner has a ring detector and if two photons are detected within short time interval, and detected opposite to each other, this suggests that a positron has been released. From this data an image of FDG accumulation is made. The PET/CT is a hybrid scanner and consists of a PET-scanner and an integrated computer tomography scanner (CT). The CT-images are superimposed on the PET images and can be used for anatomical orientation. Also, CT images are used for attenuation correction of the PET data. To measure the amount of FDG in a certain volume, the standard uptake value (SUV) is calculated as the decay-corrected tissue concentration divided by the injected dose per body weight.

PET/CT in carotid plaques

PET/CT with FDG has been used to estimate the degree of inflammation in carotid plaques. The signal correlates with the number of macrophages and foam cells in the tissue(99-101). Neovessels and loose matrix, containing smooth muscle cells and endothelial cells also correlates with the increased FDG uptake(101). It has been speculated that this could be because smooth muscle cells and endothelial cells have an increased glucose uptake when exposed to pro-inflammatory substances. The reason for increased FDG uptake in some plaques is not fully understood, there are evidence that FDG-uptake could be stimulated by the hypoxia in the plaque rather than by inflammation(102). Other data indicate that FDG uptake is associated with the presence of micro vessels, but not with markers of ongoing angiogenesis(103).

The FDG PET signal is higher in previously symptomatic plaques(104-106). Also FDG uptake is higher in carotid plaques that show micro embolic signals on transcranial Doppler examination(107). In one study, FDG uptake in previous symptomatic carotid plaques seems to be associated with risk of recurrent stroke(108). There is a need for prospective studies to establish the predictive value of FDG uptake and to gain insight into the temporal dynamics of FDG uptake in carotid plaques. As outlined, FDG uptake is affected by many mechanisms and tissues and more specific tracers are needed to clarify mechanisms of plaque vulnerability(109).

1.4.8 Spatial resolution of the different imaging modalities

Spatial resolution refers to the ability of the imaging modality to separate two objects. Of the presented methods, ultrasound has the highest spatial resolution. Resolution is dependent on which frequency is being used and resolution differs dependent on the depth of imaging. Also, the resolution of ultrasound is better in axial direction (the direction in which ultrasound is transmitted) than in the lateral direction. The maximal resolution in the ultrasound system used in this thesis is around 0.25 mm(110).

In MRI, the data is collected in a matrix and the size of the picture elements are fixed by the MRI sequence and gives an absolute limit of spatial resolution. Image resolution is a trade-off between scan-time, in plane resolution and number of slices. In the quadruple inversion recovery sequence we use voxels in the size of 0.6 x 0.6 mm and a slice thickness of 3 mm. The resulting maximum technical resolution would be 0.6 mm in the image plane, but due but due to motion the resolution is a bit less.

PET data is also collected in a matrix and reformatted to match the CT images. PET has a lower spatial resolution than ultrasound and MRI at around 7-10 mm.

2 AIM

Despite all new imaging methods in carotid artery disease, the degree of stenosis is the clinically used parameter to decide if a patient will benefit from carotid surgery and the only diagnostic test that has passed randomized controlled trials(111,112). An imaging method that proved a higher value to predict stroke-event on an individual level would be highly desirable. An imaging method of such kind could also be used to follow plaque development in vivo, increasing the understanding of plaque biology, and be used as a read-out of the effectiveness of treatments aimed at stabilizing plaques. Plaque neovascularization is thought to be important for the development of a vulnerable plaque but there is not much solid evidence. The underlying pathophysiology of the vulnerable plaque is not clear.

Contrast enhanced ultrasound has been suggested as a tool to estimate neovascularization of carotid plaques in vivo. The general aim of this thesis was to test if CEUS could be used to detect vascularization in carotid plaques and to study the biology of plaque neovascularization in humans in vivo. The thesis aims to develop, standardize and quantify the CEUS examination of carotid plaques and to use the standardized CEUS examination to gain information on plaque vulnerability. To evaluate CEUS we compared CEUS data with PET/CT and MRI, in order to investigate associations between neovascularization and other signs of plaque vulnerability.

The specific aims of the papers included in the thesis were:

I. i/To develop and validate a standardized, reproducible and semi-automated method for CEUS examinations of carotid plaques. ii/To investigate how CEUS correlate with plaque echogenicity, measured using standard ultrasound imaging and with previous clinical events.

II. To test if there is an association between plaque inflammation measured with PET/CT and vascularization measured by CEUS.

III. To determine the relationship between the level of plaque vascularization and MRI derived markers of vulnerability; size of the lipid rich necrotic core and presence of IPH.

IV. To test the performance of high resolution MRI in detecting non-stenotic carotid plaques identified using ultrasound and to answer the following questions: i/ Can MRI visualize all carotid plaques detected by ultrasound?; ii/ How does plaque height measured using ultrasound compare to plaque

height measured using MRI?; iii/ Does plaque size on ultrasound, expressed as total plaque area or maximal plaque height, correlate with total plaque volume on MRI.

3 PATIENTS AND METHODS

3.1 Subjects

The subjects in Paper I, II and III are recruited from the Western region Initiative to Gather Information on Atherosclerosis (WINGA) database. This database includes patients at Sahlgrenska University Hospital undergoing ultrasound examination for suspected cerebrovascular disease. We also invited volunteers aged 68-73 years (identified through official registers) to screening for carotid artery atherosclerosis. Eleven of the subjects in Paper II have been included in Paper I. Twenty-seven of the subjects in Paper III have also been included in Paper I. All 13 of the subjects in Paper II are included in Paper III.

The subjects of Paper IV were recruited from the SCAPIS pilot study, a population study recruiting subjects from the general population(18).

3.2 Paper I – Evaluation of CEUS

In Paper I the CEUS protocol and the analysis software program (Contrast Quantification Program, CQP) was carefully tested. The CQP was tested against visual assessment by two blinded reviewers. Reproducibility of the examination and analysis was tested in two ways. Inter-scan reproducibility was tested by re-examining subjects after 30 minutes. The reproducibility of reading images was tested when the same examination was analyzed twice.

3.2.1 Development of CEUS protocol

Different aspects of the CEUS methodology were carefully tested in pilot experiments before data collection of Paper I was started. CEUS was performed in subjects with carotid plaques of different sizes. It became clear that the plaque height on B-mode ultrasound needed to be at least 2.5 mm; otherwise the plaque could be difficult to visualize when contrast agent arrived in vessel lumen. The contrast agent in the lumen “bleeds” over onto the tissue. Also, dose of contrast agent and ultrasound system image parameters were tested. A MI of 0.06 was chosen to maintain integrity of contrast bubbles.

We early identified acoustic shadows in the plaque (due to calcifications) as a problem. The low MI used in CEUS could not visualize a contrast agent

signal from areas behind such calcifications. To handle this problem we excluded all subjects that had more than 10% of the plaque area shadowed.

3.2.2 Development of the CQP

The development and validation of the CQP is described in Paper I. A number of different ways to quantify presence of contrast agent in the plaques were tested. We used a testing platform in which different areas or pixels of the plaque could be analyzed and applied different filters and weightings. Whereas signal strength in vessel lumen rose and gradually declined over time the contrast agent in the plaque appeared as binary blinks of bright spots inside the tissue. Training and validation of the CQP followed standard guidelines for development of pattern recognition software programs(113). Different time-intensity thresholds were used and the highest correlation with visual assessment was obtained when we defined pixels as white if their intensity was >35 at least 14% of the time. The CQP expresses the degree of vascularization as CQP value. The CQP value can be an integer from 0 to 100, and is defined, as the percentages of plaque area in which contrast agent has been present.

3.3 Paper II – CEUS and inflammation

All subjects fasted 6h or more before the PET/CT examination. FDG was administrated intravenously (2.7 MBq/kg body weight). Subjects then rested for 90 minutes and were then examined in supine position. The head was resting in a fixation device during imaging. The PET/CT protocol included a low-dose radiation CT for attenuation correction. After the PET acquisition a contrast-enhanced CT-angiography was performed. This was reformatted and matched to PET data, and PET images were fused with CT angiography to enable a good visualization of carotid vessels. Presence of FDG in the carotid plaque was measured, as tissue background index (TBI) were the SUV from the plaque is divided with SUV from the blood pool, in this case from multiple measuring points in the jugular vein. We defined TBI^{MEAN} as mean of three mean SUVs within the plaque divided by mean of seven mean SUVs from the jugular vein. We defined TBI^{MAX} as the mean of three maximum SUVs within the plaque divided by mean of seven maximum SUVs from the jugular vein. To ensure that SUV in the plaque was measured in the same part of the plaque that was covered by CEUS we used a novel orientation method, developed and described in Paper II. Briefly, axial B-mode ultrasound images were used to determine the angle between the line joining the center of the external and internal carotid artery. This angle was then

transferred to axial MRI slices to find the same image plane (see Figure in Paper II).

3.4 Paper III – CEUS and LRNC

We used MRI as an *in vivo* method to gain understanding on how different plaque components correspond to different degrees of contrast-agent uptake on CEUS. To do this as accurate as possible we used our novel orientation method from Paper II. Using this, we evaluated the different plaque components in a small sector of the plaque, corresponding to the slice imaged by ultrasound. Also, the whole plaque was analyzed on MRI and volumes were calculated manually. Data on plaque volume, size of LRNC, calcifications and IPH was derived as describe in the introduction and in Paper III.

3.5 Paper IV - Detection of plaques

In Paper IV we compared the sensitivity of ultrasound and MRI to detect plaques. The Mannheim consensus provides a clear definition of a plaque on ultrasound(49), however on MRI there is no clear definition. In Paper IV, a plaque on MRI was defined as a local thickening of the vessel wall compared to normal vessel wall either within one axial slice or between two axial slices. The wall thickening should not be explained by a partial volume effect. This definition was based on visual assessment of images. The definition appeared robust since measurements of wall thickness in normal arteries were well separated from the wall thickness in the areas defined as having plaques. Importantly, this definition excludes thickening due to partial volume effects.

Ultrasound and MRI images were reviewed blinded by different readers. Number of plaques were counted in the different vessels and plaque height, plaque area (ultrasound) and plaque volume (MRI) were measured. The ultrasound image assessment was restricted to the volume covered by the MRI examination.

3.6 Ethical considerations

The studies in this thesis conform with the declaration of Helsinki. All studies were approved by the regional ethics board. Study II was also approved by the local radiation committee. All subjects gave written informed consent.

3.7 Statistics

In all papers the level of significance was set at p-values <0.05 , two sided tests, unless otherwise stated. Non-parametric tests were used when normal distribution could not be assumed.

4 RESULTS

4.1 Paper I – Evaluation of CEUS

The main result from Paper I is that our method for performing and evaluating CEUS in carotid plaques is reproducible and correlates with visual assessment. The final set for validation against visual assessment consisted of 43 plaques from 41 subjects. Visual assessment correlated with CQP values ($r = 0.68$, $p < 0.001$), Figure 1A. Reproducibility was tested in 20 subjects, both as repeated analysis of a single examination and as analysis of first and second contrast agent examination, separated by 30 minutes washout. There were no systematic differences and both analyses showed high intra class correlation (0.99 and 0.94 respectively).

We found a positive correlation between echogenicity expressed as GSM and CQP value ($r = 0.50$, $p < 0.01$). Finally, subjects with history of ipsilateral stroke or TIA had significantly higher CQP values in their carotid plaques (Figure 1B).

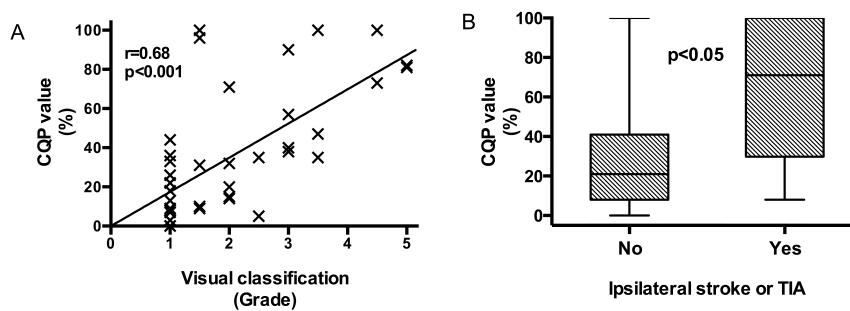


Figure 1. A: Correlation between CQP value and visual classification. B: CQP value is higher in subjects with previously ipsilateral stroke or TIA. From Hjelmgren et al. (EJVES)(79). Reprinted with permission from the publisher.

4.2 Paper II – CEUS and inflammation

The main finding of Paper II is that plaque vascularization correlates with level of inflammation in the plaque, measured with PET/CT and FDG in vivo (Figure 2). In Paper II we examined 13 subjects. Of these, 6 were previously asymptomatic, 6 had a history of stroke or TIA and 1 subject had a history of ipsilateral stroke. Median time between CEUS and PET/CT was 7 days, in one subject the time interval was 89 days. There were no differences in CQP value, GSM or TBI between previously symptomatic and non-symptomatic subjects. CQP values correlated with both TBI^{MEAN} and TBI^{MAX} . In agreement with Paper I, CQP values correlated positively with GSM also in this sub-sample ($r=0.67$, $p<0.02$). There was no correlation between GSM and TBI^{MEAN} or TBI^{MAX} .

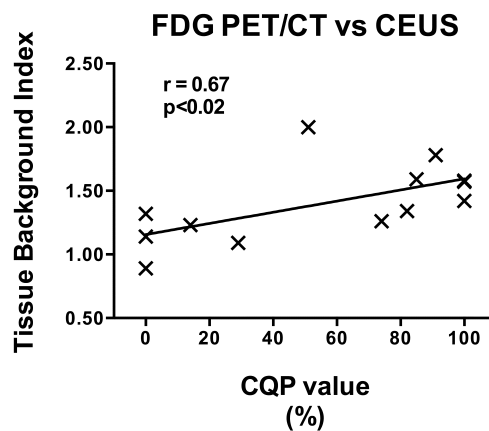


Figure 2. Plaque neovascularization correlates with the degree of plaque inflammation measured as FDG uptake in PET/CT. From Hjelmgren et al (EJR)(114) Reprinted with permission from the publisher.

4.3 Paper III – CEUS and LRNC

The most interesting finding in Paper III is that plaque vascularization is associated with a lower content of lipid rich necrotic core. In Paper III we challenged the finding in Paper I suggesting that plaque vascularization is associated with a lower content of lipid and hemorrhage as measured using ultrasound. In Paper III, 31 subjects were imaged using MRI and CEUS to further test this potential association. Median time between CEUS and MRI was 28 days. Fraction of LRNC correlated inversely with CQP value both in whole plaque and sector analysis (both analysis $r = -0.40$, $p = 0.03$), (Figure 3A). In MRI analysis of the whole plaque there were no correlations between GSM and fraction of lipid-rich necrotic core, fibrous tissue or calcifications. In sector analysis however, GSM correlated negatively with LRNC (Figure 3B) and positively with fibrous tissue ($r = -0.44$, $p = 0.01$). CQP values were similar in plaques with and without IPH.

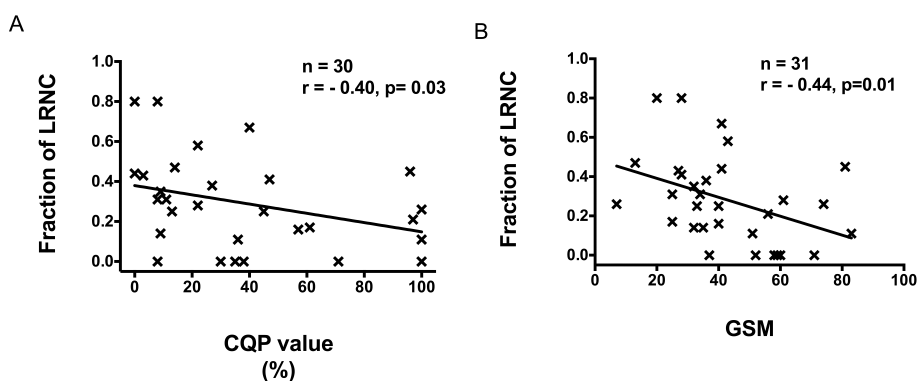


Figure 3. A: Plaque vascularization correlated negative with size of LRNC both in sector analysis (shown) and whole plaque analysis (not shown). B: Negative correlation between echogenicity (GSM) and size of LRNC when examined in sector analysis

4.4 Paper IV – Detection of plaques

The main finding of Paper IV is that MRI is comparable to ultrasound in finding plaques 2.5 mm or higher, but performs inferior to ultrasound in smaller plaques. A total of 38 subjects and 76 carotid arteries were included in the analysis. MRI detected 95% of all plaques with a height of at least 2.5 mm on ultrasound. MRI detected 53% of all ultrasound detected plaques smaller than 2.5 mm. In 25 carotid arteries, ultrasound detected two plaques were MRI only detected one plaque. In 20 of these cases, it could be shown that the ultrasound image plane cuts the same plaque twice (Figure 4). Plaque height measured on ultrasound had a similar correlation to MRI derived total plaque volume ($r=0.52, p<0.0001$) as ultrasound plaque area ($r=0.47, p<0.001$).

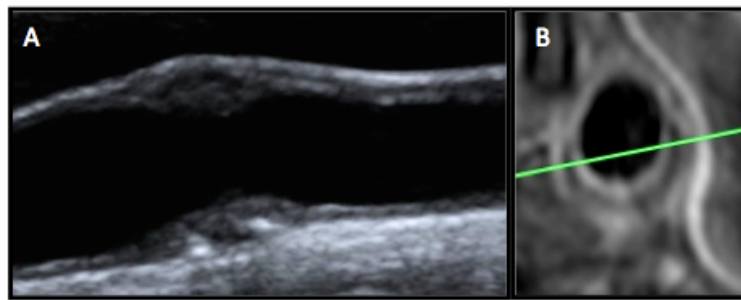


Figure 4. A: Longitudinal B-mode ultrasound image of the carotid bulb. Plaques are seen in both near and far wall. B: Axial T1 post gadolinium image of the same subject, green line shows ultrasound image plane. Note how the two plaques shown on ultrasound are in fact two parts of the same plaque.

5 DISCUSSION

5.1 Major findings in Paper I-III

When planning the first paper our first intention was to study the performance of CQP against histologic assessment of vascularization. Histologic verification would be the best way to validate our quantification software program. However, for this patient group the time from admission to the hospital to surgery is short, the median time from onset of symptoms to surgery in our hospital is 7 days(115), and enrollment of a sufficient number of subjects was not feasible. Instead we choose to test the CQP algorithm against visual assessment. Visual assessment of contrast agent uptake has been used in numerous studies providing evidence that it gives a valid approximation of plaque vascularization measured using histology(63-75).

In this thesis we have described a standardized protocol for CEUS examination and a semi-automatic quantification software program to analyze the images. We have shown that we can generate reproducible results and we have shown that data from the semi-automatic tool, CQP, correlates with visual assessment of contrast agent uptake. The output variable, CQP value, is higher in earlier symptomatic subjects than asymptomatic subjects. The distribution of CQP value is skewed towards low values, 44% of the plaques had CQP values below 20%. Accumulation of low echogenic plaques in our material could explain this finding.

Interestingly, plaques with higher GSM value have a higher CQP-value in our material. This is contradictory to most previous publications(65,66,70,76,78,83), while a few other studies fail to show any correlation between CEUS and echogenicity(42,73). We believe that the previous studies that showed an inverse correlation between echogenicity and vascularization suffers from inclusion bias since heavily calcified plaques were included. In some studies the proportion of heavily calcified plaques were as high as 25%(65). From our own experience (and explained by acoustic shadowing), little or no contrast agent can be visualized in these plaques. The shadows from a calcified near wall plaque will also affect vessel lumen and make contrast agent detection impossible. This has also been discussed by Xiong et al(76) and ten Kate et al(116). To deal with this issue we choose to exclude all subjects with more than 10% shadowing. This selection in our material led to an enrichment of subjects with low GSM.

Previous studies using histology have shown that plaques with low echogenicity/low GSM on ultrasound have a large content of lipid and a high frequency of IPH (51,54-58). In Paper III, as expected we found that the size of LRNC on MRI correlated inversely with plaque GSM. This relation was only found when the MRI images were analyzed in the sector of the plaque that corresponded to the image plane used by ultrasound. To study these relationships our newly developed orientation system is most likely critical in order to transfer information between 2D ultrasound images and volume imaging with MRI(114). Only very strong associations can be demonstrated if a 2D image is compared directly with information from a 3D volume of a heterogeneous tissue.

When comparing CEUS data of vascularization with MRI data of plaque composition we also found that plaques with more extensive vascularization had a lower content of lipid rich necrotic core measured on MRI. This was true both in sector analysis as well as when the whole plaque was analyzed on MRI suggesting a strong and solid association. This is an interesting and also contradictive finding since both large LRNC and plaque vascularization are considered as markers of vulnerability. On the other hand it is in line with our own finding that vascularization correlates positively with GSM(79). To summarize; We have shown that vascularization is higher at higher GSM values and that vascularization is higher when the LRNC is small. This means that a plaque cannot have a large LRNC and be fully vascularized. The explanation is most likely that the dead and necrotic tissue in the LRNC(5) is not vascularized and therefore ultrasound contrast agent is not distributed to this volume. This does not exclude an important role of neovascularization in plaque vulnerability. It may very well be that the important neovascularization exists in a small part of the plaque and that qualitative differences between different vessels contributes more to its role in vulnerability(39,117).

Our material shows a higher degree of neovascularization in subjects with prior symptoms and this is consistent with the majority of earlier studies(66,68,70,76-78). This supports CEUS as a marker of vulnerability but we believe that this finding must be interpreted with caution since the measurements is performed after the event. Increased vascularization could be associated with the healing of a plaque after rupture(118). The healing process in other tissues involves angiogenesis(119) and it is therefore possible that the increased vascularization observed in these types of studies is a phenomenon related to plaque healing after an event. To resolve this issue we think it is important for future studies to investigate the natural course of development of plaque morphology after an event. There is also

other evidence for a role of vascularization in development of events. Two studies have compared the grade of neovascularization in subjects with and without micro embolic signals (MES) when examined with transcranial Doppler(80,81). These findings supports the role of CEUS as a marker of vulnerability since the presence of MES is associated with increased stroke risk.

In Paper III we found no differences in vascularization between plaques with and without IPH. This finding was somewhat surprising since the mechanism behind IPH is extravasation of blood from ruptured neovessels. Also there was no difference in size of LRNC between subjects with and without IPH. These findings are not in line with findings in previous cross-sectional, histology studies on advanced carotid plaques(37) and coronary plaques(6). The discrepancy may be explained by the limited number of observations in our study. It is also important to remember that CEUS measures the quantity of vascularization, not the quality of the vessels.

In Paper II we show that plaque vascularization correlates with inflammation when measured in vivo. This supports previous histological data (39,99-101) and to our knowledge this is the first time this is shown in vivo. FDG uptake in carotid plaques is considered a marker of plaque inflammation although its specificity has recently been challenged. FDG uptake correlates with the number of foam cells and macrophages(99-101). However, tissues like loose matrix, neovessels and smooth muscle cells are also associated with elevated FDG(101). A possible explanation for the uptake in these cells is an increased cell metabolism when exposed to pro-inflammatory substances(101). Furthermore, in vitro experiments have shown that hypoxia directly can stimulate FDG uptake(102). Other data indicate that FDG uptake is associated with the presence of micro vessels, but not with markers of ongoing angiogenesis(103). Although FDG seems to be an unspecific marker, there is a common thread that increased FDG uptake is associated with different indices of plaque vulnerability.

The FDG signal in relation to the LRNC is not very well studied. In one recent work on ex-vivo plaques(101), plaques with high FDG signal did not differ in lipid core size to plaques with low FDG signal. But in most works on FDG and carotid plaque histology, data on FDG enrichment in LRNC has not been reported.

5.1.1 Applicability of CEUS

For recruitment, we screened subjects in the ages 68-73 year old. In this age interval the incidence of carotid plaques (height $\geq 2,5$ mm) in this general population was around 7%. Around 32% were then excluded due to extensive calcifications leading to acoustic shadowing (>10%). It is important to have these figures in mind when discussing the value of CEUS in a general population. CEUS of carotid plaques is a method limited to patients with at least moderate sized plaques with little acoustic shadowing. If proved valuable this technic could be used for risk stratification in this group.

5.1.2 Quantification of CEUS

An automated and objective quantification that expresses the vascularization as a continuous variable is of course a method superior to visual grading.

We tested different analysis strategies in our development platform, including variables that measured enhanced intensity and time to peak intensity. However the use of these different calculations, based on time intensity curves in the plaque relative the lumen was not robust. Some basic features of the contrast agent make this sort of analysis less suitable; a single micro bubble can be detected and will be presented as a bright spot. This makes the relation between vessel density and pixel intensity complicated and we cannot assume that the signal intensity is linear to the density of vessels present in a certain region. Single pixels showed an on/off behavior when for example a single bubble entered and exited the ultrasound image slice.

It was also evident that the quantification algorithm needed to handle both spatial and temporal resolution. The CQP algorithm looks at every pixel separately; if the pixel goes bright for a certain duration (eg. time threshold) it is considered to coincide with a vessel, even if it later turns black. The thresholds for intensity and duration were set in a training set as described in Paper I. The same strategy has been used by others in to recent works, presenting quantification software programs that works in a similar way to ours(74,120). In the paper by Zhang a software program is tested directly against histology showing good performance(74).

When conducting CEUS examinations we learned that different subjects show different signal strength from ultrasound contrast agent both in vessel lumen and in tissue, despite our attempts to standardize the examination. This phenomenon is well known from standard B-mode ultrasound and is

explained by variations in the acoustic impedance between subjects. In order to make the CEUS examination as standardized as possible we choose to scale the gray scale levels in a linear way. We used the darkest pixel in the image series as black reference and the brightest pixel in vessel lumen as white reference.

The CQP value can be an integer from 0 to 100, and is defined, as the percentages of plaque area in which contrast agent has been present for a given amount of time. After this normalization and filtering of data the CQP value could be handled as a continuous variable.

Pseudo enhancement

The pseudo enhancement artifact has been described as increased intensity in areas remote to large vessels containing contrast agent(84). There is currently no consensus on how to handle this artifact. In the works by van der Oord, the authors choose to only examine plaques in the near wall(121,122). However, in all works comparing CEUS with histology(63-75), no such restriction has been made. In Paper I we observed an increased CEUS signal in the far wall compared with the near wall. It is possible that this is explained by pseudo enhancement.

The prospective value of CEUS

There are no prospective studies to clarify if neovascularization assessed non-invasively by CEUS actually can predict future stroke or TIA. However a recent study showed that CEUS and plaque height can predict cardiac events in a high risk population with known stable coronary heart disease(123). To show that CEUS can predict stroke, large multi-center studies are probably needed. Before this is done, consensus on performance and interpretation of the examination is needed.

5.2 Differences between 2D ultrasound and MRI – Paper IV

The validity and applicability of the studies using multi modality imaging such as in Paper III is highly dependent on the sensitivity of different modalities to detect atherosclerotic plaques. To further explore this we choose to compare the two imaging methods, ultrasound and MRI, in Paper IV.

When using our novel orientation method, comparing ultrasound derived data to MRI data it became obvious that most plaques are heterogenic and

that the 2D ultrasound image plane not always is representative for the plaque morphology as seen in 3D MRI. Our very experienced sonographers were carefully instructed to obtain ultrasound image plane that would cut perpendicular through the highest part of the plaque. However, when the image plane was superimposed on the axial MRI images it became clear that ultrasound sometimes misses the most affected part of the vessel wall. These findings lead to the formulation of the research question of Paper IV.

There is no consensus of what constitutes a plaque on MRI. To be able to compare the two modalities we defined a plaque on MRI as a local thickening of the vessel wall compared to normal vessel wall either within one axial slice or between two axial slices, a thickening not explained by a partial volume effect. In an attempt to validate this visual assessment we also measured the wall thickness in sections defined as normal wall and plaque tissue respectively. This validation turned out successful with no observed overlap between the two measurements (thickness of normal wall ranged from 0.6-1.1 mm, plaque thickness was always ≥ 1.6 mm).

In Paper IV we showed that smaller plaques are easier to discover on ultrasound compared with MRI. However, plaques with a height of at least 2.5 mm on ultrasound were detected by MRI in 95% of the cases. In smaller plaques MRI only detected 53% of the ultrasound verified plaques. This is of course expected since ultrasound has a considerably higher resolution than MRI. However, in 2 cases MRI found plaques in cases where ultrasound reported no plaques. This is probably explained by the fact that the ultrasound operator cannot choose the insonation angle of the probe freely. For physical reasons, the lack of a proper perpendicular border surface, ultrasound has problems to detect plaques located in the sidewalls. In conclusion, the empiric cut off level of 2.5 mm used in several MRI studies (18,124) seems to be adequately chosen.

In Paper IV, ultrasound visualized what appeared to be two separate plaques in 27 carotid arteries. After scrutiny of MRI images, it is likely that in 20 of these cases the two plaques on ultrasound is in fact the same plaque cut twice (Figure 4). This analysis was made possible since we could project the ultrasound image plane on to MRI images using our new orientation method.

In our data, we believe that the best parameter to assess plaque burden on ultrasound is the plaque height. It shows a strong agreement with MRI assessed plaque height when the plaques are ≥ 2.5 mm and fair agreement below 2.5 mm. Plaque height and plaque area (on ultrasound) correlates similar to MRI assessed plaque volume. However, plaque height is a much

more robust and also fairly straightforward measure compared with plaque area.

We found a poor agreement when we compared the exact localization of maximum height measurement on MRI and ultrasound. Only 31% the height measurement was found within the same 90-degree sector of the vessel wall. This is not surprising since the sidewalls are hard to view on ultrasound. MRI on the other hand can view the whole circumference with equal resolution.

Interestingly, and in line with other studies(19), when the distribution of the location of maximum plaque height on MRI was plotted, as an angle from external carotid artery, it was not randomly distributed. It is much more common that the maximum plaque height is found opposite to the external carotid artery. The reason for this skewed distribution is thought to be the differences in flow hemodynamics since the turbulent flow along the outer wall induces less shear stress (20).

6 CONCLUSION

CEUS examination of carotid plaques can be performed in a standardized fashion and the examination can be quantified semi-automatically using our novel software program. CEUS can visualize the degree of vascularization in carotid plaques.

More dense vascularization is seen in plaques with a small lipid rich necrotic core, measured by MRI or as a low GSM. From this finding we speculate that the relation between the degree of neovessels and risk of plaque rupture is not simply positive. The signal from CEUS does not differentiate between mature and normally developed vessels in stable parts of the plaque and immature fragile vessels that may rupture and cause intra plaque hemorrhage.

The degree of plaque vascularization is associated with the degree of plaque inflammation measured with FDG.

MRI is equally sensitive to ultrasound in finding plaques that are 2.5 mm or higher, in smaller plaques MRI is less sensitive. Ultrasound derived plaque height is in our opinion a good proxy for MRI derived plaque volume.

Multiple plaques seen on ultrasound are often a misinterpretation of the anatomy; most often it is different parts of the same plaque visualized in different imaging planes.

7 FUTURE PERSPECTIVES

The ultrasound system and the software programs integrated in the ultrasound system needs to be technically improved. Especially the image handling of calcified tissues needs to be improved. With better technology, CEUS would be feasible in a higher number of subjects with improved image quality. The limited applicability is currently the bottleneck for the CEUS technology, not the quantification of the examination. Objective quantification is in our opinion rather good on images of reasonable quality.

To understand the pathophysiological process that leads to plaque rupture, the ideal experimental design would be to image carotid plaques the days or weeks before a rupture. In this way, plaque composition and vascularization preceding rupture could be imaged and analyzed. However, this study design is most likely utopia. The design would involve imaging of an enormous amount of subjects since only a small fraction of the subjects will suffer an event in the following week after an examination. This would be the case even if a very high-risk population were recruited. An alternative and much more feasible strategy would be to perform serial imaging after an event to capture changes in plaque morphology in the healing phase.

It would be very interesting to conduct a CEUS study of plaque vascularization targeting specific areas of the plaque. A possible design would involve initial imaging with MRI where the size and location of plaque components can be visualized. These images are then used as input in an orientation system, and CEUS is targeted against the most interesting parts of the plaque; including regions outside but close to the LRNC as well as shoulder regions. We believe that the extent of neovascularization needs to be measured in the context of the local environment. Very interesting new multi-modality imaging systems for fusion of ultrasound and various tomographic image data, like CT or MRI, is promising, since they can be used to visualize the location of the ultrasound image plane onto a MRI image in real time.

Currently, CEUS cannot tell us anything about the quality of the neovessels, only the quantity. A CEUS study using micro bubbles labeled with a tracer, that binds to molecular markers of fragile endothelium could provide image information on only the most vulnerable vessels, prone to cause IPH.

ACKNOWLEDGEMENT

Jag vill tacka alla som bidragit till min doktorsavhandling.

Ett stort tack till min huvudhandledare Göran Bergström. Jag är mycket tacksam att jag fått möjlighet att ägna mig åt forskning och att skriva denna avhandling. Det har varit ett väldigt stimulerande, utvecklande och roligt arbete.

Tack Caroline Schmidt, min bihandledare, för all hjälp med stort och smått.

Tack Lars Johansson, min bihandledare, för all hjälp med MR och PET, och för bra förklaringar av svåra saker.

Tack Ulrica Prahlgullberg, Peter Holdfeldt, Birgitta Jannemark, Marie-Louise Ekholm, Josefin Kjell Dahl, Sven-Göran Johansson, Björn Fagerberg, Lisbeth Winberg, Lotta Lord och Rosie Perkins för all hjälp och uppmuntran.

Ett stort tack till alla studiedeltagare.

Tack till Johan Fredén Lindqvist, Jakob Himmelman och Ann-Christin Berg för hjälpen med PET/CT undersökningarna.

Tack till Maria Broad Wikström, Lena Strid, Hans Klingenstierna och Anders Berntsson på Aleris röntgen för gott samarbete med MR-undersökningarna.

Tack alla kollegor på Klinisk Fysiologi Sahlgrenska och tack till mina chefer Björn Wall och Peter Gjertsson.

Jag vill tacka min familj, Mona, Ture, Ellen, Calle och Matilda, för allt stöd och all uppmuntran jag fått.

Sist men inte minst vill jag tacka Camilla för all kärlek, stöd och omtanke och Hugo för att du finns.

REFERENCES

1. Strong K, Mathers C, Bonita R. Preventing stroke: saving lives around the world. *The Lancet Neurology* 2007;6:182-7.
2. Sary HC, Blankenhorn DH, Chandler AB et al. A definition of the intima of human arteries and of its atherosclerosis-prone regions. A report from the Committee on Vascular Lesions of the Council on Arteriosclerosis, American Heart Association. *Circulation* 1992;85:391-405.
3. Chen YX, Nakashima Y, Tanaka K, Shiraishi S, Nakagawa K, Sueishi K. Immunohistochemical expression of vascular endothelial growth factor/vascular permeability factor in atherosclerotic intimas of human coronary arteries. *Arterioscler Thromb Vac Biol* 1999;19:131-9.
4. Fogelstrand P, Boren J. Retention of atherogenic lipoproteins in the artery wall and its role in atherogenesis. *Nutrition, metabolism, and cardiovascular diseases : NMCD* 2012;22:1-7.
5. Bentzon JF, Otsuka F, Virmani R, Falk E. Mechanisms of plaque formation and rupture. *Circ Res* 2014;114:1852-66.
6. Kolodgie FD, Gold HK, Burke AP et al. Intraplaque hemorrhage and progression of coronary atheroma. *N Engl J Med* 2003;349:2316-25.
7. Moore KJ, Tabas I. Macrophages in the pathogenesis of atherosclerosis. *Cell* 2011;145:341-55.
8. Sary HC, Chandler AB, Dinsmore RE et al. A definition of advanced types of atherosclerotic lesions and a histological classification of atherosclerosis. A report from the Committee on Vascular Lesions of the Council on Arteriosclerosis, American Heart Association. *Circulation* 1995;92:1355-74.
9. Kragel AH, Reddy SG, Wittes JT, Roberts WC. Morphometric analysis of the composition of atherosclerotic plaques in the four major epicardial coronary arteries in acute myocardial infarction and in sudden coronary death. *Circulation* 1989;80:1747-56.
10. Sary HC. The development of calcium deposits in atherosclerotic lesions and their persistence after lipid regression. *Am J Cardiol* 2001;88:16e-19e.
11. Otsuka F, Sakakura K, Yahagi K, Joner M, Virmani R. Has our understanding of calcification in human coronary

- atherosclerosis progressed? *Arterioscler Thromb Vac Biol* 2014;34:724-36.
12. Otsuka F, Finn AV, Virmani R. Do vulnerable and ruptured plaques hide in heavily calcified arteries? *Atherosclerosis* 2013;229:34-7.
 13. Sluimer JC, Gasc JM, van Wanroij JL et al. Hypoxia, hypoxia-inducible transcription factor, and macrophages in human atherosclerotic plaques are correlated with intraplaque angiogenesis. *J Am Coll Cardiol* 2008;51:1258-65.
 14. Sluimer JC, Kolodgie FD, Bijnens AP et al. Thin-walled microvessels in human coronary atherosclerotic plaques show incomplete endothelial junctions relevance of compromised structural integrity for intraplaque microvascular leakage. *J Am Coll Cardiol* 2009;53:1517-27.
 15. Kannel WB, McGee D, Gordon T. A general cardiovascular risk profile: the Framingham Study. *Am J Cardiol* 1976;38:46-51.
 16. Bjorck L, Rosengren A, Bennett K, Lappas G, Capewell S. Modelling the decreasing coronary heart disease mortality in Sweden between 1986 and 2002. *Eur Heart J* 2009;30:1046-56.
 17. Giang KW, Bjorck L, Novak M et al. Stroke and coronary heart disease: predictive power of standard risk factors into old age--long-term cumulative risk study among men in Gothenburg, Sweden. *Eur Heart J* 2013;34:1068-74.
 18. Bergstrom G, Berglund G, Blomberg A et al. The Swedish CARDioPulmonary BioImage Study: objectives and design. *J Intern Med* 2015.
 19. Zarins CK, Giddens DP, Bharadvaj BK, Sottiurai VS, Mabon RF, Glagov S. Carotid bifurcation atherosclerosis. Quantitative correlation of plaque localization with flow velocity profiles and wall shear stress. *Circ Res* 1983;53:502-14.
 20. Harloff A. Carotid plaque hemodynamics. *Interventional neurology* 2012;1:44-54.
 21. Parikh R, Kadowitz PJ. Angina pectoris: current therapy and future treatment options. *Expert Rev Cardiovasc Ther* 2014;12:175-86.
 22. Powers WJ. Cerebral hemodynamics in ischemic cerebrovascular disease. *Ann Neurol* 1991;29:231-40.
 23. Davies MJ. The pathophysiology of acute coronary syndromes. *Heart* 2000;83:361-6.
 24. Jashari F, Ibrahimi P, Nicoll R, Bajraktari G, Wester P, Henein MY. Coronary and carotid atherosclerosis:

- similarities and differences. *Atherosclerosis* 2013;227:193-200.
25. Libby P, Pasterkamp G. Requiem for the 'vulnerable plaque'. *Eur Heart J* 2015.
 26. Redgrave JN, Lovett JK, Gallagher PJ, Rothwell PM. Histological assessment of 526 symptomatic carotid plaques in relation to the nature and timing of ischemic symptoms: the Oxford plaque study. *Circulation* 2006;113:2320-8.
 27. Galis ZS, Sukhova GK, Lark MW, Libby P. Increased expression of matrix metalloproteinases and matrix degrading activity in vulnerable regions of human atherosclerotic plaques. *J Clin Invest* 1994;94:2493-503.
 28. Libby P. The molecular mechanisms of the thrombotic complications of atherosclerosis. *J Intern Med* 2008;263:517-27.
 29. Kolodgie FD, Burke AP, Farb A et al. The thin-cap fibroatheroma: a type of vulnerable plaque: the major precursor lesion to acute coronary syndromes. *Curr Opin Cardiol* 2001;16:285-92.
 30. Naghavi M, Libby P, Falk E et al. From vulnerable plaque to vulnerable patient: a call for new definitions and risk assessment strategies: Part I. *Circulation* 2003;108:1664-72.
 31. Hansson GK, Libby P, Tabas I. Inflammation and plaque vulnerability. *J Intern Med* 2015.
 32. Ribatti D, Levi-Schaffer F, Kovanen PT. Inflammatory angiogenesis in atherogenesis--a double-edged sword. *Ann Med* 2008;40:606-21.
 33. Virmani R, Kolodgie FD, Burke AP et al. Atherosclerotic plaque progression and vulnerability to rupture: angiogenesis as a source of intraplaque hemorrhage. *Arterioscler Thromb Vac Biol* 2005;25:2054-61.
 34. Doyle B, Caplice N. Plaque neovascularization and antiangiogenic therapy for atherosclerosis. *J Am Coll Cardiol* 2007;49:2073-80.
 35. Bjornheden T, Levin M, Evaldsson M, Wiklund O. Evidence of hypoxic areas within the arterial wall in vivo. *Arterioscler Thromb Vac Biol* 1999;19:870-6.
 36. Sluimer JC, Daemen MJ. Novel concepts in atherogenesis: angiogenesis and hypoxia in atherosclerosis. *J Pathol* 2009;218:7-29.
 37. McCarthy MJ, Loftus IM, Thompson MM et al. Angiogenesis and the atherosclerotic carotid plaque: an association between symptomatology and plaque morphology. *J Vasc Surg* 1999;30:261-8.

38. Taqueti VR, Di Carli MF, Jerosch-Herold M et al. Increased microvascularization and vessel permeability associate with active inflammation in human atheromata. *Circulation Cardiovascular imaging* 2014;7:920-9.
39. Jeziorska M, Woolley DE. Local neovascularization and cellular composition within vulnerable regions of atherosclerotic plaques of human carotid arteries. *J Pathol* 1999;188:189-96.
40. Hellings WE, Peeters W, Moll FL et al. Composition of carotid atherosclerotic plaque is associated with cardiovascular outcome: a prognostic study. *Circulation* 2010;121:1941-50.
41. van Hinsbergh VW, Eringa EC, Daemen MJ. Neovascularization of the atherosclerotic plaque: interplay between atherosclerotic lesion, adventitia-derived microvessels and perivascular fat. *Curr Opin Lipidol* 2015.
42. Kim HS, Woo JS, Kim BY et al. Biochemical and clinical correlation of intraplaque neovascularization using contrast-enhanced ultrasound of the carotid artery. *Atherosclerosis* 2014;233:579-83.
43. Saam T, Hetterich H, Hoffmann V et al. Meta-analysis and systematic review of the predictive value of carotid plaque hemorrhage on cerebrovascular events by magnetic resonance imaging. *J Am Coll Cardiol* 2013;62:1081-91.
44. Mofidi R, Crotty TB, McCarthy P, Sheehan SJ, Mehigan D, Keaveny TV. Association between plaque instability, angiogenesis and symptomatic carotid occlusive disease. *Br J Surg* 2001;88:945-50.
45. Flaherty ML, Kissela B, Khoury JC et al. Carotid artery stenosis as a cause of stroke. *Neuroepidemiology* 2013;40:36-41.
46. Otto C. Principles of echocardiographic image acquisition and doppler analysis. *Textbook of clinical echocardiography*, 2009:1-29.
47. Turner SP, Monaghan MJ. Tissue harmonic imaging for standard left ventricular measurements: fundamentally flawed? *European journal of echocardiography : the journal of the Working Group on Echocardiography of the European Society of Cardiology* 2006;7:9-15.
48. Jogestrand T, Lindqvist M, Nowak J. Diagnostic performance of duplex ultrasonography in the detection of high grade internal carotid artery stenosis. *Eur J Vasc Endovasc Surg* 2002;23:510-8.
49. Touboul PJ, Hennerici MG, Meairs S et al. Mannheim carotid intima-media thickness and plaque consensus (2004-

- 2006-2011). An update on behalf of the advisory board of the 3rd, 4th and 5th watching the risk symposia, at the 13th, 15th and 20th European Stroke Conferences, Mannheim, Germany, 2004, Brussels, Belgium, 2006, and Hamburg, Germany, 2011. *Cerebrovasc Dis* 2012;34:290-6.
50. Gray-Weale AC, Graham JC, Burnett JR, Byrne K, Lusby RJ. Carotid artery atheroma: comparison of preoperative B-mode ultrasound appearance with carotid endarterectomy specimen pathology. *J Cardiovasc Surg (Torino)* 1988;29:676-81.
 51. Sztajzel R, Momjian S, Momjian-Mayor I et al. Stratified gray-scale median analysis and color mapping of the carotid plaque: correlation with endarterectomy specimen histology of 28 patients. *Stroke* 2005;36:741-5.
 52. Elatrozy T, Nicolaidis A, Tegos T, Zarka AZ, Griffin M, Sabetai M. The effect of B-mode ultrasonic image standardisation on the echodensity of symptomatic and asymptomatic carotid bifurcation plaques. *Int Angiol* 1998;17:179-86.
 53. Sabetai MM, Tegos TJ, Nicolaidis AN, Dhanjil S, Pare GJ, Stevens JM. Reproducibility of computer-quantified carotid plaque echogenicity: can we overcome the subjectivity? *Stroke* 2000;31:2189-96.
 54. Carotid artery plaque composition--relationship to clinical presentation and ultrasound B-mode imaging. European Carotid Plaque Study Group. *Eur J Vasc Endovasc Surg* 1995;10:23-30.
 55. El-Barghouty NM, Levine T, Ladva S, Flanagan A, Nicolaidis A. Histological verification of computerised carotid plaque characterisation. *Eur J Vasc Endovasc Surg* 1996;11:414-6.
 56. Gronholdt ML, Wiebe BM, Laursen H, Nielsen TG, Schroeder TV, Sillesen H. Lipid-rich carotid artery plaques appear echolucent on ultrasound B-mode images and may be associated with intraplaque haemorrhage. *Eur J Vasc Endovasc Surg* 1997;14:439-45.
 57. Gronholdt ML, Nordestgaard BG, Bentzon J et al. Macrophages are associated with lipid-rich carotid artery plaques, echolucency on B-mode imaging, and elevated plasma lipid levels. *J Vasc Surg* 2002;35:137-45.
 58. Sztajzel R. Ultrasonographic assessment of the morphological characteristics of the carotid plaque. *Swiss medical weekly* 2005;135:635-43.
 59. Mathiesen EB, Bonna KH, Joakimsen O. Echolucent plaques are associated with high risk of ischemic cerebrovascular

- events in carotid stenosis: the tromso study. *Circulation* 2001;103:2171-5.
60. Gronholdt ML, Nordestgaard BG, Schroeder TV, Vorstrup S, Sillesen H. Ultrasonic echolucent carotid plaques predict future strokes. *Circulation* 2001;104:68-73.
61. Piscaglia F, Bolondi L. The safety of Sonovue in abdominal applications: retrospective analysis of 23188 investigations. *Ultrasound Med Biol* 2006;32:1369-75.
62. Phillips P, Gardner E. Contrast-agent detection and quantification. *Eur Radiol* 2004;14 Suppl 8:P4-10.
63. Shah F, Balan P, Weinberg M et al. Contrast-enhanced ultrasound imaging of atherosclerotic carotid plaque neovascularization: a new surrogate marker of atherosclerosis? *Vasc Med* 2007;12:291-7.
64. Vicenzini E, Giannoni MF, Puccinelli F et al. Detection of carotid adventitial vasa vasorum and plaque vascularization with ultrasound cadence contrast pulse sequencing technique and echo-contrast agent. *Stroke* 2007;38:2841-3.
65. Coli S, Magnoni M, Sangiorgi G et al. Contrast-enhanced ultrasound imaging of intraplaque neovascularization in carotid arteries: correlation with histology and plaque echogenicity. *J Am Coll Cardiol* 2008;52:223-30.
66. Giannoni MF, Vicenzini E, Citone M et al. Contrast carotid ultrasound for the detection of unstable plaques with neoangiogenesis: a pilot study. *Eur J Vasc Endovasc Surg* 2009;37:722-7.
67. Hoogi A, Adam D, Hoffman A, Kerner H, Reisner S, Gaitini D. Carotid plaque vulnerability: quantification of neovascularization on contrast-enhanced ultrasound with histopathologic correlation. *AJR Am J Roentgenol* 2011;196:431-6.
68. Faggioli GL, Pini R, Mauro R et al. Identification of carotid 'vulnerable plaque' by contrast-enhanced ultrasonography: correlation with plaque histology, symptoms and cerebral computed tomography. *Eur J Vasc Endovasc Surg* 2011;41:238-48.
69. Shalhoub J, Monaco C, Owen DR et al. Late-phase contrast-enhanced ultrasound reflects biological features of instability in human carotid atherosclerosis. *Stroke* 2011;42:3634-6.
70. Varetto G, Gibello L, Bergamasco L et al. Contrast enhanced ultrasound in atherosclerotic carotid artery disease. *Int Angiol* 2012;31:565-71.
71. Vavuranakis M, Sigala F, Vrachatis DA et al. Quantitative analysis of carotid plaque vasa vasorum by CEUS and

- correlation with histology after endarterectomy. *Vasa* 2013;42:184-95.
72. Muller HF, Viaccoz A, Kuzmanovic I et al. Contrast-enhanced ultrasound imaging of carotid plaque neovascularization: accuracy of visual analysis. *Ultrasound Med Biol* 2014;40:18-24.
 73. Li C, He W, Guo D et al. Quantification of carotid plaque neovascularization using contrast-enhanced ultrasound with histopathologic validation. *Ultrasound Med Biol* 2014;40:1827-33.
 74. Zhang Q, Li C, Han H et al. Spatio-temporal Quantification of Carotid Plaque Neovascularization on Contrast Enhanced Ultrasound: Correlation with Visual Grading and Histopathology. *Eur J Vasc Endovasc Surg* 2015.
 75. Iezzi R, Petrone G, Ferrante A et al. The role of contrast-enhanced ultrasound (CEUS) in visualizing atherosclerotic carotid plaque vulnerability: which injection protocol? Which scanning technique? *Eur J Radiol* 2015;84:865-71.
 76. Xiong L, Deng YB, Zhu Y, Liu YN, Bi XJ. Correlation of carotid plaque neovascularization detected by using contrast-enhanced US with clinical symptoms. *Radiology* 2009;251:583-9.
 77. Huang PT, Chen CC, Aronow WS et al. Assessment of neovascularization within carotid plaques in patients with ischemic stroke. *World journal of cardiology* 2010;2:89-97.
 78. Owen DR, Shalhoub J, Miller S et al. Inflammation within carotid atherosclerotic plaque: assessment with late-phase contrast-enhanced US. *Radiology* 2010;255:638-44.
 79. Hjelmgren O, Holdfeldt P, Johansson L et al. Identification of vascularised carotid plaques using a standardised and reproducible technique to measure ultrasound contrast uptake. *Eur J Vasc Endovasc Surg* 2013;46:21-8.
 80. Zhou Y, Xing Y, Li Y et al. An assessment of the vulnerability of carotid plaques: a comparative study between intraplaque neovascularization and plaque echogenicity. *BMC medical imaging* 2013;13:13.
 81. Ritter MA, Theismann K, Schmiedel M, Ringelstein EB, Dittrich R. Vascularization of carotid plaque in recently symptomatic patients is associated with the occurrence of transcranial microembolic signals. *Eur J Neurol* 2013;20:1218-21.
 82. Markus HS, King A, Shipley M et al. Asymptomatic embolisation for prediction of stroke in the Asymptomatic Carotid Emboli Study (ACES): a prospective observational study. *The Lancet Neurology* 2010;9:663-71.

83. Huang PT, Huang FG, Zou CP et al. Contrast-enhanced sonographic characteristics of neovascularization in carotid atherosclerotic plaques. *J Clin Ultrasound* 2008;36:346-51.
84. ten Kate GL, Renaud GG, Akkus Z et al. Far-wall pseudoenhancement during contrast-enhanced ultrasound of the carotid arteries: clinical description and in vitro reproduction. *Ultrasound Med Biol* 2012;38:593-600.
85. Thapar A, Shalhoub J, Averkiou M, Mannaris C, Davies AH, Leen EL. Dose-dependent artifact in the far wall of the carotid artery at dynamic contrast-enhanced US. *Radiology* 2012;262:672-9.
86. Westbrook C, Kaut-Roth C, Talbot J. *MRI in practice*, 2012.
87. Kerwin WS, Zhao X, Yuan C et al. Contrast-enhanced MRI of carotid atherosclerosis: dependence on contrast agent. *J Magn Reson Imaging* 2009;30:35-40.
88. Saam T, Ferguson MS, Yarnykh VL et al. Quantitative evaluation of carotid plaque composition by in vivo MRI. *Arterioscler Thromb Vac Biol* 2005;25:234-9.
89. Cai J, Hatsukami TS, Ferguson MS et al. In vivo quantitative measurement of intact fibrous cap and lipid-rich necrotic core size in atherosclerotic carotid plaque: comparison of high-resolution, contrast-enhanced magnetic resonance imaging and histology. *Circulation* 2005;112:3437-44.
90. Yuan C, Kerwin WS, Ferguson MS et al. Contrast-enhanced high resolution MRI for atherosclerotic carotid artery tissue characterization. *J Magn Reson Imaging* 2002;15:62-7.
91. Wasserman BA, Smith WI, Trout HH, 3rd, Cannon RO, 3rd, Balaban RS, Arai AE. Carotid artery atherosclerosis: in vivo morphologic characterization with gadolinium-enhanced double-oblique MR imaging initial results. *Radiology* 2002;223:566-73.
92. Hatsukami TS, Ross R, Polissar NL, Yuan C. Visualization of fibrous cap thickness and rupture in human atherosclerotic carotid plaque in vivo with high-resolution magnetic resonance imaging. *Circulation* 2000;102:959-64.
93. Mitsumori LM, Hatsukami TS, Ferguson MS, Kerwin WS, Cai J, Yuan C. In vivo accuracy of multisequence MR imaging for identifying unstable fibrous caps in advanced human carotid plaques. *J Magn Reson Imaging* 2003;17:410-20.
94. Ota H, Yarnykh VL, Ferguson MS et al. Carotid intraplaque hemorrhage imaging at 3.0-T MR imaging: comparison of the diagnostic performance of three T1-weighted sequences. *Radiology* 2010;254:551-63.

95. Takaya N, Yuan C, Chu B et al. Association between carotid plaque characteristics and subsequent ischemic cerebrovascular events: a prospective assessment with MRI--initial results. *Stroke* 2006;37:818-23.
96. Yuan C, Zhang SX, Polissar NL et al. Identification of fibrous cap rupture with magnetic resonance imaging is highly associated with recent transient ischemic attack or stroke. *Circulation* 2002;105:181-5.
97. Yarnykh VL, Yuan C. T1-insensitive flow suppression using quadruple inversion-recovery. *Magn Reson Med* 2002;48:899-905.
98. Moody AR, Murphy RE, Morgan PS et al. Characterization of complicated carotid plaque with magnetic resonance direct thrombus imaging in patients with cerebral ischemia. *Circulation* 2003;107:3047-52.
99. Tawakol A, Migrino RQ, Bashian GG et al. In vivo 18F-fluorodeoxyglucose positron emission tomography imaging provides a noninvasive measure of carotid plaque inflammation in patients. *J Am Coll Cardiol* 2006;48:1818-24.
100. Tawakol A, Migrino RQ, Hoffmann U et al. Noninvasive in vivo measurement of vascular inflammation with F-18 fluorodeoxyglucose positron emission tomography. *J Nucl Cardiol* 2005;12:294-301.
101. Liu J, Kerwin WS, Caldwell JH et al. High resolution FDG-microPET of carotid atherosclerosis: plaque components underlying enhanced FDG uptake. *Int J Cardiovasc Imaging* 2015.
102. Folco EJ, Sheikine Y, Rocha VZ et al. Hypoxia but not inflammation augments glucose uptake in human macrophages: Implications for imaging atherosclerosis with 18fluorine-labeled 2-deoxy-D-glucose positron emission tomography. *J Am Coll Cardiol* 2011;58:603-14.
103. Pedersen SF, Graebe M, Hag AM, Hoejgaard L, Sillesen H, Kjaer A. Microvessel density but not neoangiogenesis is associated with 18F-FDG uptake in human atherosclerotic carotid plaques. *Molecular imaging and biology : MIB : the official publication of the Academy of Molecular Imaging* 2012;14:384-92.
104. Skagen K, Johnsrud K, Evensen K et al. Carotid plaque inflammation assessed with (18) F-FDG PET/CT is higher in symptomatic compared with asymptomatic patients. *International journal of stroke : official journal of the International Stroke Society* 2015;10:730-6.

105. Rudd JH, Warburton EA, Fryer TD et al. Imaging atherosclerotic plaque inflammation with [18F]-fluorodeoxyglucose positron emission tomography. *Circulation* 2002;105:2708-11.
106. Graebe M, Pedersen SF, Hojgaard L, Kjaer A, Sillesen H. 18FDG PET and ultrasound echolucency in carotid artery plaques. *JACC Cardiovasc Imaging* 2010;3:289-95.
107. Muller HF, Viacoz A, Fisch L et al. 18FDG-PET-CT: an imaging biomarker of high-risk carotid plaques. Correlation to symptoms and microembolic signals. *Stroke* 2014;45:3561-6.
108. Marnane M, Merwick A, Sheehan OC et al. Carotid plaque inflammation on 18F-fluorodeoxyglucose positron emission tomography predicts early stroke recurrence. *Ann Neurol* 2012;71:709-18.
109. Joshi NV, Vesey AT, Williams MC et al. 18F-fluoride positron emission tomography for identification of ruptured and high-risk coronary atherosclerotic plaques: a prospective clinical trial. *Lancet* 2014;383:705-13.
110. Siemens Healthcare, Personal communication. 2015.
111. Randomised trial of endarterectomy for recently symptomatic carotid stenosis: final results of the MRC European Carotid Surgery Trial (ECST). *Lancet* 1998;351:1379-87.
112. Rothwell PM, Eliasziw M, Gutnikov SA, Warlow CP, Barnett HJ. Endarterectomy for symptomatic carotid stenosis in relation to clinical subgroups and timing of surgery. *Lancet* 2004;363:915-24.
113. Bergström G, Prah U, Holdfeldt P. Automated classification of plaques. In: Nicolaides AB, K.W.; Kyriacou, E.; Pattichis, C.S., editor *Ultrasound and Carotid Bifurcation Atherosclerosis*, 2012.
114. Hjelmgren O, Johansson L, Prah U, Schmidt C, Freden-Lindqvist J, Bergstrom GM. A study of plaque vascularization and inflammation using quantitative contrast-enhanced US and PET/CT. *Eur J Radiol* 2014;83:1184-9.
115. Stromberg S, Nordanstig A, Bentzel T, Osterberg K, Bergstrom GM. Risk of early recurrent stroke in symptomatic carotid stenosis. *Eur J Vasc Endovasc Surg* 2015;49:137-44.
116. Ten Kate GL, van den Oord SC, Sijbrands EJ et al. Current status and future developments of contrast-enhanced ultrasound of carotid atherosclerosis. *J Vasc Surg* 2013;57:539-46.

117. Thim T, Hagensen MK, Bentzon JF, Falk E. From vulnerable plaque to atherothrombosis. *J Intern Med* 2008;263:506-16.
118. Olson FJ, Stromberg S, Hjelmgren O, Kjell Dahl J, Fagerberg B, Bergstrom GM. Increased vascularization of shoulder regions of carotid atherosclerotic plaques from patients with diabetes. *J Vasc Surg* 2011;54:1324-1331 e5.
119. Singer AJ, Clark RA. Cutaneous wound healing. *N Engl J Med* 1999;341:738-46.
120. Akkus Z, Hoogi A, Renaud G et al. New quantification methods for carotid intra-plaque neovascularization using contrast-enhanced ultrasound. *Ultrasound Med Biol* 2014;40:25-36.
121. van den Oord SC, Akkus Z, Roeters van Lennep JE et al. Assessment of subclinical atherosclerosis and intraplaque neovascularization using quantitative contrast-enhanced ultrasound in patients with familial hypercholesterolemia. *Atherosclerosis* 2013;231:107-13.
122. van den Oord SC, Akkus Z, Renaud G et al. Assessment of carotid atherosclerosis, intraplaque neovascularization, and plaque ulceration using quantitative contrast-enhanced ultrasound in asymptomatic patients with diabetes mellitus. *European heart journal cardiovascular Imaging* 2014;15:1213-8.
123. Nakamura J, Nakamura T, Deyama J et al. Assessment of carotid plaque neovascularization using quantitative analysis of contrast-enhanced ultrasound imaging is useful for risk stratification in patients with coronary artery disease. *Int J Cardiol* 2015;195:113-9.
124. van den Bouwhuijsen QJ, Vernooij MW, Hofman A, Krestin GP, van der Lugt A, Witteman JC. Determinants of magnetic resonance imaging detected carotid plaque components: the Rotterdam Study. *Eur Heart J* 2012;33:221-9.